

Topographic modelling in electrical imaging inversion

M.H.LOKE

A slightly updated version of an abstract submitted for the EAGE 62nd Conference and Technical Exhibition — Glasgow, Scotland, 29 May - 2 June 2000

Abstract

To invert the data obtained from 2-D electrical imaging surveys (Griffiths and Barker 1993), a cell based model which consists of a large number of rectangular blocks is commonly used (Loke and Barker 1996). This model (Figure 1a) consists of a number of horizontal layers that are subdivided into rectangular blocks by vertical boundaries. The inversion program then determines the resistivity of the blocks that will best reproduce the measured apparent resistivity values. The finite-difference or finite-element method is used to calculate the apparent resistivity values for the resistivity model. The smoothness-constrain least squares method (deGroot-Hedlin and Constable 1990, Ellis and Oldenburg 1994) is frequently used to carry out the inversion. The equation used by this method is given by

$$(\mathbf{J}^T\mathbf{J} + u\mathbf{F})\mathbf{d} = \mathbf{J}^T\mathbf{g} - u\mathbf{F}\mathbf{r} \quad (1)$$

where \mathbf{F} is a smoothing matrix, \mathbf{J} is the Jacobian matrix of partial derivatives, \mathbf{r} is a vector containing the logarithm of the model resistivity values, u is a damping factor, \mathbf{d} is the model perturbation vector and \mathbf{g} is a vector containing the differences between the logarithms of the measured and calculated apparent resistivity values.

It is well known that surface topography can have a significant effect on the resistivity measurements (Tsourles *et al.* 1999). For accurate interpretation, the effect of the topography must be accounted for in some way. One common method is the "topographic corrections" method where the apparent resistivity values for a homogeneous earth model with the observed topography is calculated. The ratio of the true resistivity to the calculated apparent resistivity values for the homogenous model is then multiplied with the measured apparent resistivity values (Fox *et al.* 1980). In theory, this method is exact if the subsurface below the survey line is also homogeneous. Since the actual subsurface geology is always inhomogeneous, the calculated correction factors are at best approximate. The errors in the inversion results introduced by the use of the corrections factors depend on the nature of the topography as well as the subsurface resistivity distribution. If there are large resistivity contrasts near the surface, this method could cause significant distortions in the inversion results (Tong and Yang 1990).

The "topographic corrections" method attempts to interpret the data collected over a real earth with topography using a model with a flat surface. By using the finite-element method (Silvester and Ferrari 1990) for the forward modelling calculations, a model where the surface nodes are shifted up or down to match the actual topography can be used. The topography is directly incorporated into the inversion model (Tong and Yang 1990) which eliminates the need to carry out the "topographic corrections". The time taken by the finite-element forward modelling subroutine depends on the number of the nodes used but it is independent of the shape of the mesh. Thus the "topographic modelling" method does not require any additional computational time.

Figure 1 shows three possible schemes to implement this method which differ in the way the subsurface nodes are shifted to accommodate the surface topography. The simplest approach (Figure 1b) is to shift all the subsurface nodes by the same amount as the surface node along the same vertical mesh line (Sasaki *et al.*, 1992; Sasaki 1994). This is probably acceptable for cases with a small to moderate topographic variation. In the second method, the amount the subsurface

nodes are shifted is reduced in an exponential manner with depth (Figure 1c) such that at a sufficiently great depth the nodes are not shifted (Holcombe and Jirack 1984). This comes from the observation that the effect of the topography is reduced or damped with depth. One possible way to implement this method is by the following equation,

$$\Delta z_j = T_i \exp(-k z_j / (T_m + H_m - T_i)) \quad (2)$$

where Δz_j is the vertical shift in the node coordinate, z_j is the depth of the node below the surface in the original undistorted grid (Figure 1a), T_i is the surface elevation, T_m is difference in elevation between the highest and lowest topography points, H_m is the elevation of the highest point and k is a constant (normally equals to 1) which controls the degree of damping. This method produces a more pleasing model section (Figure 1c with k equals to 1) than the first method in that every kink in the surface topography is not reproduced in all the layers. For data sets where the topography has moderate curvature, this is a robust and simple method. One disadvantage of this method is that it can produce a model with unusually thick layers below sections where the topography curves upwards (hills), and thin layers where the topography curves downwards (valleys) if a large damping factor is used (Figure 1d with k equals to 3). Thus the model obtained is also dependent on the degree of damping selected.

In the third method, the inverse Schwartz-Christoffel transformation is used to calculate shift needed for the subsurface nodes. The Schwartz-Christoffel transformation method was used by Spiegel *et al.* (1980) to transform a model with topography into an equivalent model with a flat surface. In this paper, the inverse transform is used to transform the original model with a flat surface (Figure 1a) into a model with topography (Figure 1e). Since this method also takes into account the curvature of the surface topography, it can avoid some of the pitfalls of the second method with a damped distorted grid.

Figure 2 shows the inversion results from a survey across the Ratchrogan Mound in Ireland (Waddell and Barton 1995) that contains significant topography. Note that the inverse Schwartz-Christoffel transformation model (Figure 2d) avoids the bulge near the middle of the line produced by the model with a damped distorted grid (Figure 2c).

References

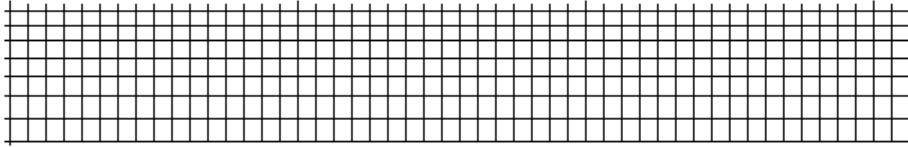
- deGroot-Hedlin, C. and Constable, S., 1990. Occam's inversion to generate smooth, two-dimensional models from magnetotelluric data. *Geophysics*, **55**, 1613-1624.
- Ellis, R.G. and Oldenburg, D.W., 1994. Applied geophysical inversion. *Geophysical Journal International*, **116**, 5-11.
- Fox, R., Hohmann, G., Killpack, T. and Rjio, L., 1980. Topographic effects in resistivity and induced polarization surveys. *Geophysics*, **45**, 75-93.
- Griffiths D.H. and Barker R.D., 1993. Two-dimensional resistivity imaging and modelling in areas of complex geology. *Journal of Applied Geophysics*, **29**, 211-226.
- Holcombe, J. and Jirack, G., 1984. 3-D terrain corrections in resistivity surveys. *Geophysics*, **49**, 439-452.
- Loke M.H. and Barker R.D., 1996. Rapid least-squares inversion of apparent resistivity pseudosections using a quasi-Newton method. *Geophysical Prospecting*, **44**, 131-152.
- Sasaki, Y., Yoneda, Y. and Matsuo, K., 1992. Resistivity imaging of controlled-source audiofrequency magnetotelluric data. *Geophysics*, **57**, 952-955.
- Sasaki, Y., 1994. 3-D resistivity inversion using the finite-element method. *Geophysics*, **59**, 1839-1848.
- Silvester P.P. and Ferrari R.L., 1990. Finite elements for electrical engineers (2nd. ed.). Cambridge University Press.
- Spiegel, R.J., Sturdivant, V.R. and Owen, T.E., 1980. Modeling resistivity anomalies from localized voids under irregular terrain. *Geophysics*, **45**, 1164-1183.

Tong, L. and Yang, C., 1990. Incorporation of topography into 2-D resistivity inversion. *Geophysics*, **55**, 354-361.

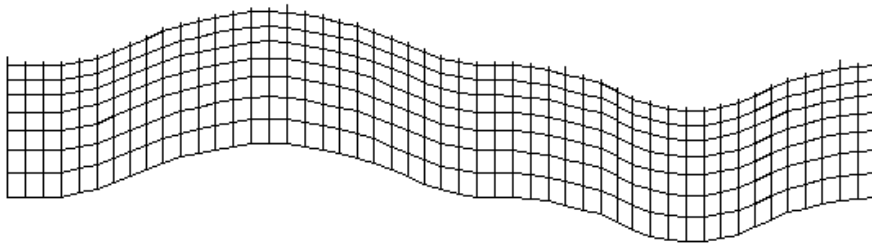
Tsourles, P.I., Symanski, J.E. and Toskas, G.N., 1999. The effect of terrain topography on commonly used resistivity arrays. *Geophysics*, **64**, 1357-1363.

Waddell, J. and Barton, K., 1995, Seeing beneath Rathcroghan. *Archaeology Ireland*, Vol. 9, No. 1, 38-41.

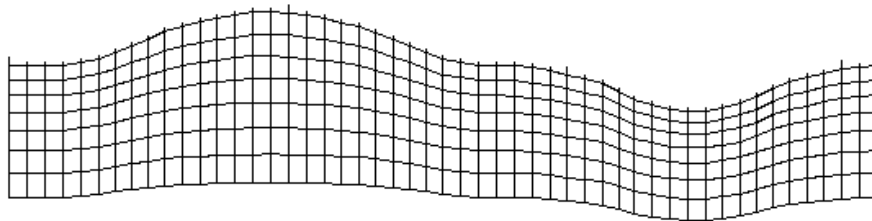
a). Arrangement of model blocks without topography



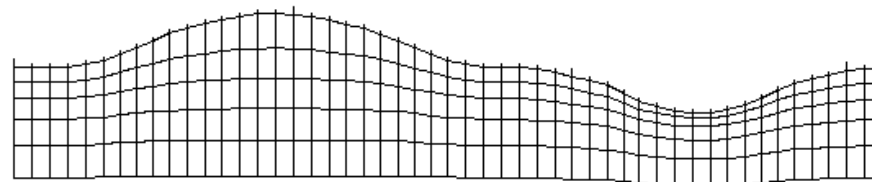
b). Arrangement of model blocks with a uniformly distorted grid



c). Arrangement of model blocks with a moderately damped distorted grid



d). Arrangement of model blocks with a highly damped distorted grid



e). Arrangement of model blocks with the inverse Schwartz-Christoffel transformation

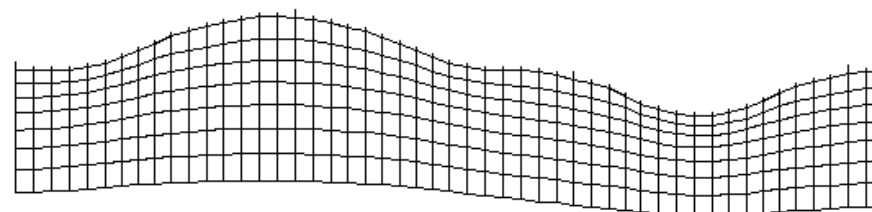
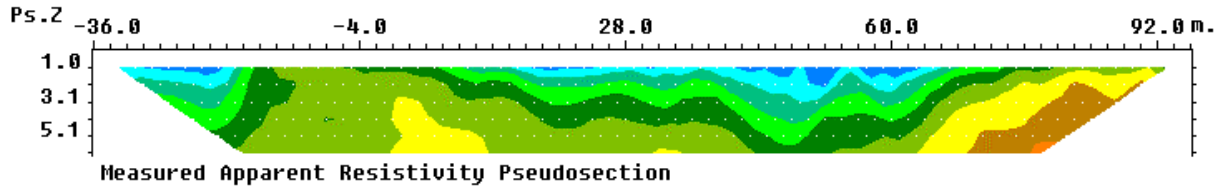


Figure 1. (a) Schematic diagram of a typical 2-D inversion model with no topography. A finite-element mesh with four nodes in the horizontal direction between adjacent electrodes is normally used. The near surface layers are also subdivided vertically by several mesh lines. Models with a distorted grid to match the actual topography where (b) the subsurface nodes are shifted vertically by the same amount as the surface nodes, (c) the shift in the subsurface nodes are gradually reduced with depth (with the damping factor k equals to 1) or (d) rapidly reduced with depth (with k equals to 3), and (e) the model obtained with the inverse Schwartz-Christoffel transformation method.

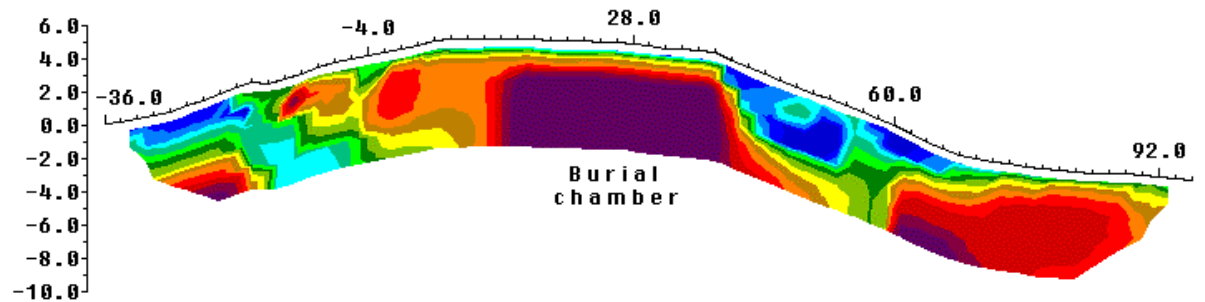
Rathcroghan Mound survey

a). Apparent resistivity pseudosection



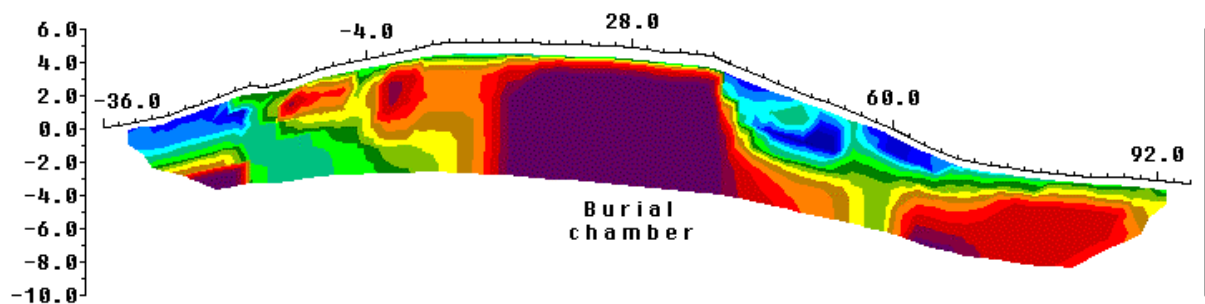
b). Uniformly distorted grid

Iteration 6 RMS error = 2.0



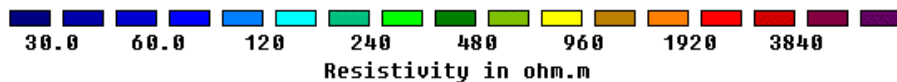
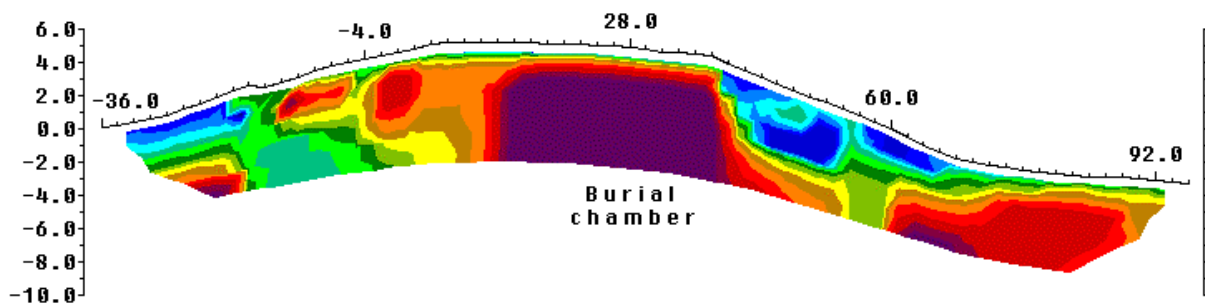
c). Damped distorted grid

Iteration 6 RMS error = 2.1



d). Inverse Schwartz-Christoffel transformation grid

Iteration 6 RMS error = 2.0



Vertical exaggeration in model section display = 2.00

Unit Electrode Spacing = 2.0 m.

Figure 2. Rathcroghan Mound survey. (a) Measured apparent resistivity pseudosection with the Wenner array. Model sections obtained after inversion using (b) a uniformly distorted grid, (c) a damped distorted grid (with the damping factor k equals to 1) and (d) a grid calculated with the inverse Schwartz-Christoffel transformation. The high resistivity body below the centre of the survey line is a burial chamber.